

The fact that the exceptional frequencies are stop frequencies is demonstrated by examining the magnitude of A . Referring to Eq. (4) above, if the argument of the logarithm exceeds unity, A is negative and the exceptional frequencies correspond to stop frequencies, i.e. $A < 0$, if

$$\left| \frac{\tilde{\omega} l_s / k_\infty}{k_2 \cos \tilde{\omega} l_r + k_1 \sin \tilde{\omega} l_r} \right| > 1$$

or

$$\tilde{\omega} l_s / k_\infty > |k_2 \cos \tilde{\omega} l_r + k_1 \sin \tilde{\omega} l_r|. \quad (9)$$

The value of the right hand side of expression (9) is bounded by zero and unity. Incorporation of the upper bound results in

$$\tilde{\omega} > \frac{k_\infty}{l_s},$$

which satisfies expression (1) for systems whose thermal-diffusion lifetime is at least as large as the slowing-down time.

Similar arguments for $A > 0$ lead to the condition

$$\tilde{\omega} < \frac{k_\infty}{l_s},$$

which violates expression (1). Thus, for bare thermal multiplying media (and within the framework of the age diffusion model) the only exceptional frequencies are stop frequencies.

The simplicity of requirement (1) is a consequence of the continuous slowing-down model employed. It is interesting and perhaps surprising that the characteristic time is the slowing-down time and not, for example, the mean time to fission. It should be emphasized, too, that the simple age-diffusion model is not necessarily valid at the high frequencies contemplated. This aspect is currently being investigated by examining the dispersion relationships obtained from a telegrapher age-diffusion model.

R. L. Brehm

University of California
at Los Angeles
Los Angeles, California

Received October 14, 1964
Revised November 24, 1964

Multilevel Cross Sections and Reactor Criticality*

Resonance cross sections of the fissile isotopes have been treated in two essentially distinct

fashions in reactor analysis. In the thermal energy range, which is normally chosen to extend from 0 to about 0.5 eV, these cross sections may be represented as empirical pointwise functions of energy. In the epithermal energy range, on the other hand, resonances are so numerous and so sharp that one must represent them analytically. Since the Breit-Wigner single-level formula¹ has been universally used in this connection, it becomes interesting to examine the effects that the approximate nature of this formula may have on criticality calculations.

One possible defect of the single-level formula is made evident by considering the fission-to-absorption ratio in a pure U²³⁵ fuel element. Near an epithermal resonance energy, E_λ , the fission and absorption of the uranium are dominated by the resonance in question, and the fission-to-absorption ratio of the fuel predicted by the single-level formula is, to a good approximation, the ratio of the partial widths for fission and absorption, $\Gamma_f^\lambda / (\Gamma_f^\lambda + \Gamma_\gamma^\lambda)$, a quantity independent of fuel-plate thickness or shape. The general Wigner-Eisenbud theory^{2,3}, on the other hand, states that

$$E^{1/2} \sigma_c = \text{const} \sum_c \left| \sum_{\lambda, \lambda'} (\Gamma_{n,o}^\lambda)^{1/2} (\Gamma_c^{\lambda'})^{1/2} A_{\lambda\lambda'} \right|^2, \quad (1)$$

where

c refers to either fission or capture channels

$$(A^{-1})_{\lambda\lambda'} = (E_\lambda - E) \delta_{\lambda\lambda'} - \frac{1}{2} i \sum_c (\Gamma_c^\lambda)^{1/2} (\Gamma_c^{\lambda'})^{1/2}$$

$\Gamma_{n,o}^\lambda$ is the reduced neutron width of the resonance at E_λ .

In agreement³ with experiment, Eq. (1), which we shall refer to as the multilevel formula, predicts that while the capture cross section σ_γ is symmetric about E_λ , the fission cross section is not. The fission-to-absorption ratio in a fuel element is thus a function of its dimensions. Since to a first approximation the effective multiplication constant of a reactor is proportional to $1/(1+\alpha)$, it becomes necessary to investigate the variation of this ratio with fuel plate geometry.

Multilevel values of $1/(1+\alpha)$ (averaged over the energy range between 0.625 and 3.7 eV) were calculated for a series of slab lattices composed of U²³⁵ fuel plates (10% by atom U²³⁵ in Zr) and water at 293°K. The Doppler-broadened multilevel cross

¹A. M. WEINBERG and E. P. WIGNER, *The Physical Theory of Neutron Chain Reactors*, University of Chicago Press, Chicago, Illinois (1958).

²E. P. WIGNER and L. EISENBUD, *Phys. Rev.*, **72**, 29 (1947).

³E. VOGT, *Phys. Rev.*, **112**, 203 (1958), and *Phys. Rev.*, **118**, 724 (1960).

*Work performed under the auspices of the USAEC.

sections were determined from Eq. (1) using Vogt's method³ of evaluating $A_{\lambda\lambda'}$. It is perhaps useful to sketch here some of the salient features of the Vogt formalism. If the matrix A^{-1} is assumed to be diagonal, Eq. (1) reduces to a sum of single-level contributions. The off-diagonal elements $(A^{-1})_{\lambda\lambda'}$ give rise to terms in Eq. (1) corresponding to interference between resonance energy levels and are of the form³

$$(A^{-1})_{\lambda\lambda'} = -(i/2)|g_{\lambda f}| |g_{\lambda' f}| I_{\lambda\lambda'} \quad (\lambda \neq \lambda'), \quad (2)$$

where the interference coefficient $I_{\lambda\lambda'}$ varies between 0 (no interference) and 1 (total interference), and $|g_{\lambda f}| = (\Gamma_f^\lambda/2)^{1/2}$. Following Vogt we introduce the fission vectors $\vec{g}_{\lambda f}$ and $\vec{g}_{\lambda' f}$ and speak of the last three quantities in Eq. (2) as their scalar product. For a set of N interfering levels one has N fission vectors one of which, $\vec{g}_{\lambda f}$, is chosen arbitrarily as polar axis. The other vectors $\vec{g}_{\lambda' f}$ may then be specified either by giving $\Gamma_f^{\lambda'}$ and $\theta_{\lambda\lambda'}$ (the angle between $\vec{g}_{\lambda f}$ and $\vec{g}_{\lambda' f}$) or, as we have done in Table I, giving directly the x and y components $|g_{\lambda f}|_x$ and $|g_{\lambda f}|_y$ of each fission vector. Figure 1 provides a comparison of the multilevel absorption cross sections with those generated from the single-level parameters in BNL-325. One notes that while the single-level formula represents peak cross sections well, it is much less successful between resonances.

Once computed for a given composition, the cross sections were stored on tape as a permanent library for neutron transport calculations. In this manner, Monte Carlo calculations⁴ of the capture and fission rates become feasible, and a method of treating the very complicated fuel element geometries that occur in actual reactors may be developed. To accelerate the calculations, resonances above 3.7 eV were ignored, and the flux above this energy was assumed to be spatially flat and to

TABLE I
Multilevel U^{235} Resonance Parameters

E_λ (eV)	Γ_f^λ (eV)	$2g\Gamma_{n,\sigma}^\lambda$ (eV)	$ g_{\lambda f} _x$ (eV)	$ g_{\lambda f} _y$ (eV)
-0.95	0.0276	0.1488×10^{-2}	0.2910	0
0.273	0.0290	0.5630×10^{-5}	0.02359	0.2209
1.140	0.0440	0.1613×10^{-4}	-0.05996	-0.2423
2.035	0.0350	0.5370×10^{-5}	fn a	fn a
3.160	0.0311	0.1823×10^{-4}	-0.1969	0.1969
3.599	0.0370	0.2430×10^{-4}	-0.03604	-0.1456

^aTreated as single-level resonance with $(\Gamma_f/2)^{1/2} = 0.0060$.

⁴N. R. CANDELORE and R. C. GAST, WAPD-TM-407 (1963).

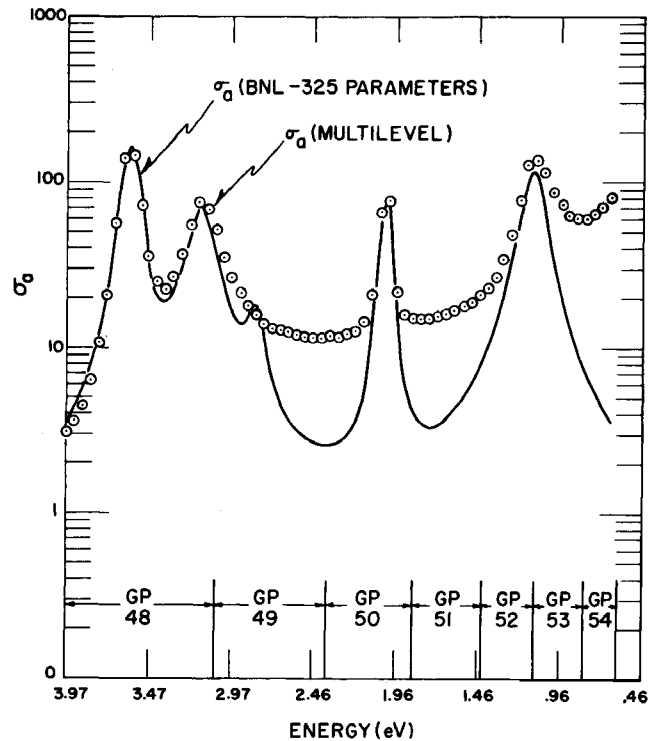


Fig. 1. Single-level and multilevel U^{235} absorption cross sections.

vary as $1/E$. Monte Carlo determinations of $1/(1+\alpha)$ are presented in Table II. It would appear that, at least over the energy range considered, the variation of $1/(1+\alpha)$ with fuel plate width may be safely neglected in all but unrealistically thick U^{235} fuel elements. Table II does, however, point up the appreciable difference in the single-level and multilevel values of $1/(1+\alpha)$ in any given lattice. This discrepancy may be removed for thin fuel plates of pure U^{235} by the addition of smooth capture and fission cross sections to the single-level cross sections. Since it is not feasible to add the smooth cross sections as pointwise functions of energy over the entire epithermal energy range of 10 MeV, one customarily divides this range into a number of multigroups (Fig. 1) and

TABLE II
Average Fission-to-Absorption Ratios ($0.625 \leq E \leq 3.7$ eV)

Width Fuel (cm)	Width Water (cm)	$\frac{1}{1+\alpha}$ (multilevel)	$\frac{1}{1+\alpha}$ (single-level)
0	∞	0.756 ± 0.001	0.836 ± 0.003
0.1	0.1	0.756 ± 0.003	---
1.0	1.0	0.755 ± 0.003	---
10.0	1.0	0.736 ± 0.002	0.837 ± 0.003

TABLE III
Variation of ρ with Parasitic Absorber Content of Fuel Plate
($0.625 \leq E \leq 1.5$ eV)

N Parasitic Absorber	$\frac{1}{1+\alpha}$ (Single-Level Formula)	$\frac{1}{1+\alpha}$ (Multilevel Formula)	ρ
0	0.885	0.815	0.921 ± 0.001
5×10^{-5}	0.407	0.401	0.986 ± 0.013
4×10^{-4}	0.132	0.129	0.982 ± 0.019
8×10^{-4}	0.0849	0.0856	1.009 ± 0.027

inserts constant average cross sections into each of these in such a manner as to reproduce the experimental values of the fission and absorption resonance integrals.

Actual reactor fuel elements, however, often contain parasitic absorbing isotopes, some of whose resonances may lie close to one or more of the U^{235} resonances. To study the behavior of the fission-to-absorption ratio under these conditions let us consider a fuel plate of composition: $N(U^{235}) = 0.002$, $N(Zr) = 0.04$, and varying amounts of a parasitic absorber whose single-level resonance parameters $E_0 = 1.1$ eV, $\Gamma_\gamma = 67$ mV, and $\Gamma_n = 2.1$ mV are chosen to emphasize interference with the U^{235} resonance at 1.14 eV. We consider once more a slab lattice composed of fuel plates and water channels, each region of which is 0.127-cm thick. Smooth fission and absorption cross sections have been added in the manner described in the last paragraph.

Values of ρ , the ratio of multilevel to single-level values of $1/(1+\alpha)$, are presented in Table III together with the probable errors in ρ deduced from the Monte Carlo output. One notes that when parasitic absorption becomes comparable to the U^{235} absorption, ρ is 6% less than its initial value; thus for fuel plates of a composition typical of pressurized-water reactors the customary addition of smooth cross sections has not reproduced the correct variation of $1/(1+\alpha)$ with parasitic absorber concentration. The evaluation of the consequent errors introduced in reactor lifetime studies will have to await the availability of multilevel parameters for a wider energy range than that considered here.

M. Goldsmith
N. R. Candelore

Bettis Atomic Power Laboratory
Westinghouse Electric Corporation
West Mifflin, Pennsylvania 15122

Received September 17, 1964
Revised December 16, 1964

A Semi-Empirical Description of the Detailed Thermal Flux Distribution in Uranium Oxide Clusters

At the present time there is no simple way of calculating the detailed fine structure in cluster fuel elements, although such elements are of increasing practical importance. Experimental knowledge of the fine structure in clusters is useful, therefore, for checking new calculational methods as well as for providing important design information. In design studies, as far as the thermal utilization is concerned, it is usually sufficient to know the relative *average* flux in each rod of a cluster. For thermodynamic studies, on the other hand, one often needs the two-dimensional flux distribution at each rod position, or the 'hyperfine structure.' In clusters of more than a few rods the determination of the complete hyperfine structure becomes quite tedious so that it would be useful to find an analytic expression for such distributions depending on a few easily measured quantities.

At Saclay we have measured the fine structure in a number of natural uranium oxide clusters of the type commonly used in gas-cooled, D_2O - or graphite-moderated reactors¹. In two of these clusters the hyperfine structure was measured in detail.

The first was composed of 19 UO_2 rods of 12-mm-diam clad in 1-mm-thick aluminum. A central rod is surrounded by two concentric rings (6 rods at a radius of 19 mm and 12 at 37 mm). The second was made up of seven 22-mm-diam rods similarly clad. Six rods surround a central rod at a radius of 32 mm. Both clusters were contained in a magnesium pressure tube 106 mm in diameter.

¹P. F. PALMEDO, "Etudes Experimentales de Structure Fine a l'Interieure des Grappes d'Oxyde UO_2 ," CEA Report No. 2387 (1964).